The effect of electron-phonon renormalisation on the thermoelectric power of NbN films

1989 J. Phys.: Condens. Matter 1 10107

(http://iopscience.iop.org/0953-8984/1/50/012)

J. Phys.: Condens. Matter **1** (1989) 10107–10116. Printed in the UK

The effect of electron–phonon renormalisation on the thermoelectric power of NbN films

S Reiff†‡, R Huber†, P Ziemann† and A B Kaiser§

† Fakultät Physik, Universität Konstanz, D-7750 Konstanz, Federal Republic of Germany

§ Physics Department, Victoria University of Wellington, PO Box 600, Wellington, New Zealand

Received 15 May 1989

Abstract. Sputtered polycrystalline NbN films were chosen as test material for investigating the theoretical prediction that electron–phonon renormalisation should lead to a non-linear temperature behaviour of the absolute thermoelectric power $S(T)$ of a metallic system.

For this system the influence of phonon drag can be ignored because the films have high resistivity, and the Eliashberg function containing the information on the electron–phonon coupling is known from experiment. The experimental results for $S(T)$ within the range $7.2\ \mathrm{K} \leqslant T \leqslant 300\ \mathrm{K}$ show a positive sign and a pronounced non-linear behaviour, which can be described by theory using experimentally known Eliashberg functions, corroborating the influence of electron–phonon renormalisation.

1. Introduction

The diffusion thermoelectric power of metals is almost never observed to show a linear behaviour at low temperatures, owing to the perturbing influence of several effects. In pure crystalline metals, the most significant of these is the phonon drag contribution to thermopower caused by the phonon current in the presence of a temperature gradient. However, in disordered materials, the drastic reduction in phonon mean free path means that the phonon drag thermopower is expected to be essentially eliminated (Jäckle 1980). But even in glassy metals in which phonon drag is absent, the observed behaviour of the thermopower is still not linear in temperature. A characteristic 'knee', or change in slope, is seen in the vicinity of about 50 K (Gallagher 1981, Kaiser 1982). Although other explanations have been proposed (e.g. by Egorushkin and Melnikova 1987), this non-linear thermopower behaviour is usually ascribed to the effect of the electron–phonon interaction, which renormalises the electron energy, velocity and relaxation time (Ono and Taylor 1980). In many glassy metals and Chevrel superconductors, good agreement with theoretical predictions of the electron–phonon enhancement effect has been obtained (Kaiser *et al* 1986, Compans and Baumann 1987, Kaiser 1987a). But for a quantitative comparison with theory, the Eliashberg function $\alpha^2F(E)$ giving information about the electron–phonon interaction must be known. In a superconductor this function can be principally obtained from tunnelling experiments (McMillan and Rowell 1969).

‡ Present address: Fritz Haber Institut, Bereich Oberflächenphysik, D-1000 Berlin, Federal Republic of Germany.

0953-8984/89/5010107 + 10 $02.50

In practice, however, these experiments are very often hindered by the impossibility of preparing tunnel junctions of high enough quality. Thus in the earlier work simple model functions of α^2F had to be used for the theoretical analysis (Kaiser and Stedman 1985, Naugle *et al* 1985). Only recently, for the case of amorphous alloys, an analysis was performed for the first time using experimentally determined α^2F functions (Mawdsley and Kaiser 1988), and was found to support the idea of electron–phonon renormalisation. It is the aim of the present work to extend this corroboration to crystalline samples—as in the case of Chevrel phases, but now based on an experimentally determined Eliashberg function. Thus, as a necessary prerequisite, the samples must exhibit a high enough electrical resistivity to suppress the phonon drag effect.

All the above requirements can be fulfilled by sputtered NbN films, which can be prepared in the cubic B1 phase and show high electrical resistivities due to their granular structure (Nigro *et al* 1988). Additionally, since NbN films are attractive for superconducting applications, their synthesis and superconducting properties were extensively studied, by techniques including superconducting tunnelling experiments, which uncovered the quantitative behaviour of α^2F (Geerk *et al* 1985, Kihlstrom *et al* 1985).

In contrast to the numerous studies on the superconducting and structural properties of NbN films, to our knowledge there are no results on the thermopower of such films.

Even for bulk samples only a few early results are available (Samsonov and Verkhoglyadova 1962, L'vov *et al* 1960), which report different signs of the Seebeck coefficient indicating the difficulty of preparing single δ-phase bulk samples. This lack of information served as an additional motivation of the present work.

2. Experimental details

2.1. Film preparation and characterisation

The NbN films were prepared by reactive DC magnetron sputtering onto thin (0.1 mm) glass substrates held at ambient temperature. The total pressure of the Ar/N_2 gas mixture ranged between 10 and 50 mTorr resulting in a film growth rate of about 2 nm s^{-1}. This rate fits very well into the recently found scaling relation for sputtered NbN films (Capone *et al* 1989). Film thicknesses between 200 nm and 400 nm were used. To characterise the films, the temperature dependence of their resistance $R(T)$ was determined. Depending on the detailed sputtering conditions films with resistivities $\rho(20\,\mathrm{K})$ between 200 $\mu\Omega$ cm and 500 $\mu\Omega$ cm could be prepared. These samples all exhibited a negative temperature coefficient of resistivity as indicated by the ratios $r = R(300\,\mathrm{K})/R(20\,\mathrm{K})$, which were in the range $0.7 \leqslant r \leqslant 0.95$ confirming earlier results (Bacon *et al* 1983, Nigro *et al* 1988).

Despite the high resistivity values, x-ray analysis of the films clearly revealed their polycrystallinity. Thus a structure model assuming small δ-NbN grains with low resistances in series with high-resistance barriers seems to be appropriate.

But, since no direct measurements of the grain size were performed, the resistivity variation cannot be attributed to a higher density of the grain boundaries or to a higher average resistance of each boundary. Additional evidence for this model stems from the lattice parameter measurements, which give values between 0.4386 nm and 0.4394 nm in close agreement with the bulk value of 0.4392 nm (Brauer and Kirner 1964). Despite this agreement, from EDX analysis one has to conclude that oxygen is present within the films, most probably in the form of interface oxides (Darlinski and Halbritter 1987).

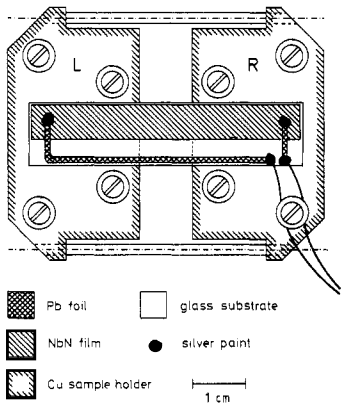

Figure 1. A top view of the thermocouple arrangement used for the $S(T)$ determination.

The $R(T)$ measurements also allow the determination of the superconducting transition temperature T_c. For the high-resistivity film ($\rho = 500\ \mu\Omega$ cm, $r = 0.7$), $T_c = 14.4$ K was found; for the low-resistivity film ($\rho = 200\ \mu\Omega$ cm, $r = 0.95$), $T_c = 16.1$ K. From the correlation between T_c and the nitrogen concentration of NbN_x (Brauer and Kirner 1964) the values $x = 0.86$ and $x = 0.92$ are obtained, respectively. From the superconducting behaviour one has to conclude that the high-resistance barriers addressed in the above model of the film structure still allow Josephson coupling of the grains.

2.2. *Measurement of the thermoelectric power*

The dynamic method that is applied for the measurement of the thermopower of the NbN films has been described recently (Compans 1989, Reiff 1988). Thus only the basic features will be mentioned in the following.

To obtain the absolute thermopower S_A of a metal A from the experimentally determined value S_{AB} of a thermocouple consisting of two metals A and B, the thermopower S_B of the reference metal must be known. Since for lead the corresponding data are available (Roberts 1977), in the following a NbN-film/Pb-foil thermocouple is always used. The experimental arrangement is shown in figure 1 giving a top view of the Cu sample holder. This holder is split into two thermally decoupled halves (L, R), each of which is equipped with its own electrical heater and thermometer (Si diodes). In this way the temperatures of the two halves can be changed and controlled separately. The substrate containing the thermocouple is glued to the holder as shown in figure 1, to provide good thermal contact. The Cu holder itself is connected to the bottom of a ^{4}He cryostat via two bronze sheets. The geometry of these sheets has to be optimised with respect to the thermal time constant of the whole arrangement, which in turn is governed by the thermal conductivity along the substrate, the thermal contact of the substrate to the Cu holder, its heat capacity and its thermal coupling to the He tank. To maintain a constant temperature gradient between the sample holder and the He tank during the course of the $S(T)$ measurement, the tank temperature could be controlled by a separate thermometer and heater.

The basic idea of the dynamic method to determine $S(T)$ is to heat one half of the sample holder, thereby increasing its temperature while the temperature of the other one is kept constant.

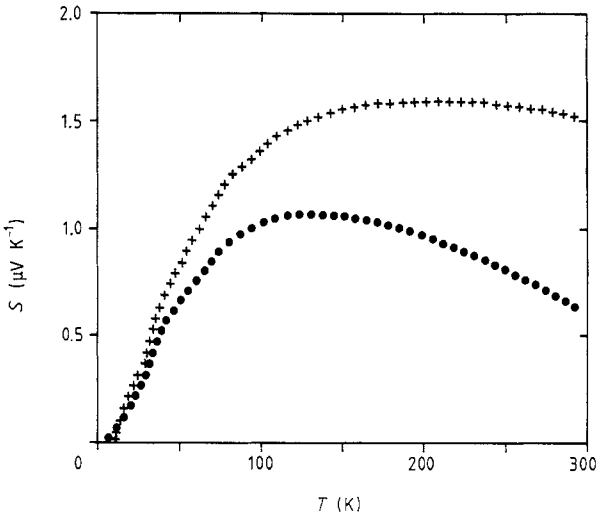

Figure 2. The absolute thermoelectric power S as a function of temperature T for two NbN_x films of different qualities (+: ρ (20 K) = 200 $\mu\Omega$ cm, T_c = 16.1 K, x = 0.92; ●: ρ (20 K) = 500 $\mu\Omega$ cm, T_c = 14.4 K, x = 0.86).

If the temperature difference ΔT developing in this way exceeds a certain upper limit, ΔT_{max}, heating of that half of the holder is stopped and the heating is switched to the other half, and so on. In this way, the average temperature of the sample is increasing linearly, while the temperature difference producing the thermoelectric signal is oscillating in a sawtooth fashion about zero. Consequently, the same behaviour is found for the thermoelectric voltage ΔU. Both signals are registered simultaneously by computer-controlled nanovoltmeters allowing us to obtain 80 data points during each heating cycle, corresponding to one specific average temperature $\bar{T}$. From a linear fit to the ΔU versus ΔT data obtained in this way, the thermopower S is deduced and attributed to $\bar{T}$. To test the above method, the absolute thermopower S_{Pb} of lead was determined within the temperature range 7.2 K $< T <$ 15 K (within this range lead conducts normally, while NbN is still superconducting with $S_{NbN} = 0$) revealing a maximum deviation from the Roberts data of 20 nV K^{-1} corresponding to about 5%. For temperatures between 15 K and 300 K the apparatus was tested by measuring the thermopower of a metallic glass against Pb and cross checking the results via an independent measurement on the same sample performed by E Compans. As a result the following limits for the relative error $\Delta S/S$ can be given. For 15 K $< T <$ 30 K one finds 2.5%, and this is followed by the range 30 K $< T <$ 60 K with the largest uncertainty of 10%. The most reliable data with an error smaller than 2% can be obtained within the range 60 K $< T <$ 300 K.

These results confirm the advantages of the dynamic method as stated recently (Compans 1989), i.e. high measuring speed, insensitivity to spurious EMFs and offset drifts.

3. Results and comparison with theory

Our main result is presented in figure 2, where the absolute thermoelectric powers of two different NbN_x films are presented as a function of temperature. The crosses

correspond to a film with $\rho = 200\ \mu\Omega$ cm, $r = 0.95$, $T_c = 16.1$ K, $x = 0.92$, while the full circles correspond to a more off-stoichiometric film with $\rho = 500\ \mu\Omega$ cm, $r = 0.7$, $T_c = 14.4$ K, $x = 0.86$. From the figure, the following main features can be deduced: the sign of the thermopower is positive for both NbN films; $S(T)$ clearly exhibits a non-linear behaviour; the film stoichiometry influences $S(T)$ significantly.

If, as in earlier work (Lye 1965), Mott's theory of the diffusion thermopower is applied to the refractory materials, the condition for a positive sign of S is given by

$$\partial \ln(N_d)/\partial E|_{E=E_F} > \tfrac{3}{2}E_F \tag{3.1}$$

where E_F is the Fermi energy and N_d is the density of states of the d band. These properties have been calculated for NbN (Dacorogna *et al* 1984) and the results are consistent with (3.1). Weak localisation due to a small electron mean free path appears to have a tendency to increase the magnitude of the thermopower (whatever its sign) as resistivity increases if other factors are constant (Kaiser 1987b). This effect, however, will be small if the initial thermopower is small, and variations in electronic structure may well dominate thermopower variations in a series of alloys. The thermopower of NbN is small, and in our case the film with the higher resistivity shows the lower $S(T)$ values indicating an influence of stoichiometry, which is more specific than the general resistivity rule quoted above. Weak localisation does not greatly affect the temperature dependence of the thermopower (Kaiser 1987b).

In the following we will restrict the discussion on the non-linear $S(T)$ behaviour to the film with the highest T_c. Experiments are in progress wherein the superconducting transition temperature is reduced by heavy-ion irradiation and the corresponding effect on the thermopower is studied. The off-stoichiometric film shown in figure 2, for comparison, will be discussed in this context elsewhere.

The metallic diffusion thermopower in the presence of the electron–phonon interaction can be written as (Kaiser 1984, Kaiser and Stedman 1985)

$$S(T) = (1 + \lambda_S(T))S_b(T) + (2\alpha + \gamma)\lambda_S(T)T. \tag{3.2}$$

Here $S_b(T)$ is the bare thermopower in the absence of the electron–phonon interaction, which is usually taken as linear in the absence of magnetic effects; $\lambda_S(T)$ is the electron–phonon enhancement factor for thermopower, which is equal to the usual mass enhancement factor λ in the limit of zero temperature; α indicates the size of the velocity and relaxation time renormalisation effects; and γ gives the contribution from higher-order diagrams (the Nielsen–Taylor effect).

The contributions from velocity and relaxation time renormalisation and from higher-order diagrams have the same temperature dependence as that from energy renormalisation in the simplest approximation for strongly disordered systems (Kaiser 1984, Kaiser and Stedman 1985), so in this case α and γ can be taken as constants.

The thermopower enhancement $\lambda_S(T)$ can be calculated if the Eliashberg function $\alpha^2F(E)$ giving information about the electron–phonon interaction is known:

$$\lambda_S(T) = \int_0^\infty \mathrm{d}E \frac{\alpha^2F(E)}{E} G_S(E/k_BT) \tag{3.3}$$

where $G_S(E/k_BT)$ is a function derived and evaluated elsewhere (Kaiser 1984).

One of the advantages of NbN is that the Eliashberg function has been determined by tunnelling measurements (Geerk *et al* 1985, Kihlstrom *et al* 1985). However, the

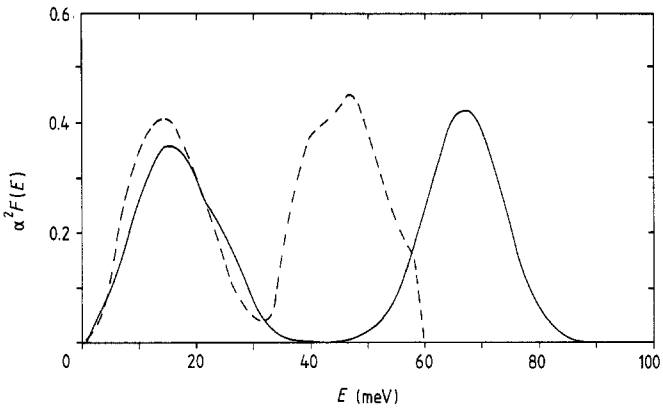

Figure 3. The Eliashberg functions α^2F, versus energy E, that were used for the calculation of $\lambda_S(T)$. The broken curve represents the data of Kihlstrom *et al* (1985); the full curve shows a model α^2F based on data obtained by Geerk *et al* (1985).

results differ markedly as regards the electron coupling to the optical phonons (above $E = 30$ meV).

The peak of α^2F obtained by Kihlstrom at 48 meV (see figure 3, broken curve) is probably due to the effect of inelastic tunnelling (Geerk *et al* 1985), since the experimentally determined phonon density of states $F(E)$ at this energy is virtually zero (Gompf and Reichardt 1975). For the calculation of $\lambda_S(T)$, we therefore use the two Eliashberg functions shown in figure 3, where the broken curve represents the data of Kihlstrom *et al* (1985).

The full curve is an α^2F function constructed in the following way. In the range $0 \leqslant E \leqslant 40$ meV the tunnelling data were taken from Geerk *et al* (1985), while for higher energies a Gaussian is used, centred at the corresponding peak of $F(E)$ as determined by neutron scattering. For the broadness of the Gaussian, the corresponding experimental value of $F(E)$ was again used, and the area was adjusted to 1.1 times the area of the low-energy part. The latter value is based on experience with ZrN, where tunnelling data are available, including the effect of optical phonons (Geerk *et al* 1986).

From the above α^2F, one obtains $\lambda = 1.19$ and $E_{\log} = 15.41$ meV ($E_{\log}$ is an average phonon energy as defined by Allen and Dynes 1975). Using the T_c formula of these authors, $T_c = 15.8$ K is obtained (assuming $\mu^* = 0.1$) in close agreement with the experimental value.

For both the Eliashberg functions shown in figure 3, $\lambda_S(T)$ was evaluated. The results are shown in figure 4, where $\overline{\lambda_S}(T)$ is $\lambda_S(T)$ normalised with its value λ at zero temperature, and are plotted to correspond to figure 3, i.e. the broken curve is based on the 'Kihlstrom α^2F' ($\lambda = 1.46$), the full curve on our 'model α^2F' ($\lambda = 1.19$). As can be seen, although the α^2F functions differ significantly above 30 meV (see figure 3), this difference is not reflected strongly in the $\overline{\lambda_S}(T)$ results. Here significant differences are only observed above 150 K, with a maximum of 16% at 300 K.

This behaviour is due to the strong weighting of the low phonon energies (see (3.3)), where both α^2F functions agree reasonably well.

A similar effect is found for $\lambda = \lambda_S(0)$: even if the coupling to the optical phonons is totally ignored and only the energy range $0 \leqslant E \leqslant 40$ meV taken into acount, the corresponding λ decreases by only 21%.

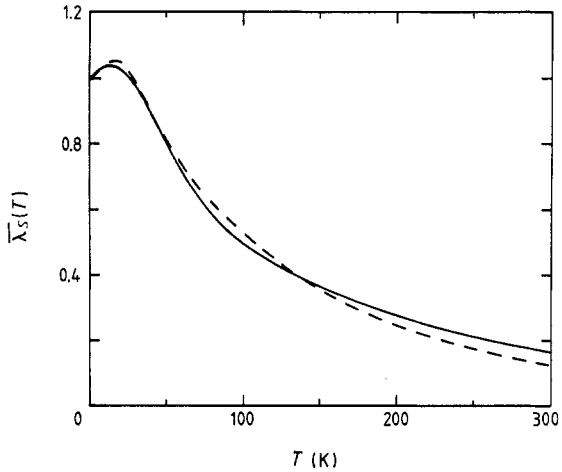

Figure 4. The temperature dependence of the normalised electron–phonon coupling constant $\overline{\lambda_S}(T)$ as given by equation (3.3). The broken curve was obtained for the Kihlstrom data, the full curve for the model α^{xe}

We now compare the experimental data for the thermopower of NbN (above the transition temperature) with the following expression:

$$S(T) = X_b T + c\overline{\lambda_S}(T)T \tag{3.4}$$

where the constant c is given by

$$c = (X_b + 2\alpha + \gamma)\lambda. \tag{3.5}$$

The temperature dependences of the terms in equation (3.4) are fixed but their magnitudes are least-squares-fitted to the data. The resulting comparison of theory and experiment is shown in figure 5. The observed non-linearity of the thermopower is of the general shape predicted by the inclusion of the effects of the electron–phonon interaction. We note the occurrence of the 'knee' at a significantly higher temperature (approximately 100 K) than for many other systems. We suggest that the reason for this is that the lattice vibration energies (and so Debye temperature) in NbN are relatively large.

The root mean square energy for the Eliashberg function $\alpha^2F(E)$ of Kihlstrom *et al* (1985) is approximately 36 meV, corresponding to a temperature of about 420 K, and the Debye temperature of a Debye spectrum with the same root mean square energy is about 540 K, the corresponding values for our model α^2F are even higher (50 meV and 750 K for the Debye temperature).

Turning now to the values of the fitting parameters, we note that the value of the bare thermopower parameter X_b is small ($X_b = 3.4$ nV K^{-2} for the Kihlstrom data and $X_b = 2.4$ nV K^{-2} for the model α^2F). As mentioned, there is a statistical tendency for the magnitude of the thermopower to increase with resistivity, but the value of X_b for a particular system depends on electronic structure. We conclude that in NbN the energy dependence of electronic structure in the immediate vicinity of the Fermi surface is likely to be weak.

The large values of the parameter c in the fits of figure 5 ($c = 17.7$ nV K^{-2} for the Kihlstrom data and $c = 19.7$ nV K^{-2} for the model α^2F) indicate that it cannot be

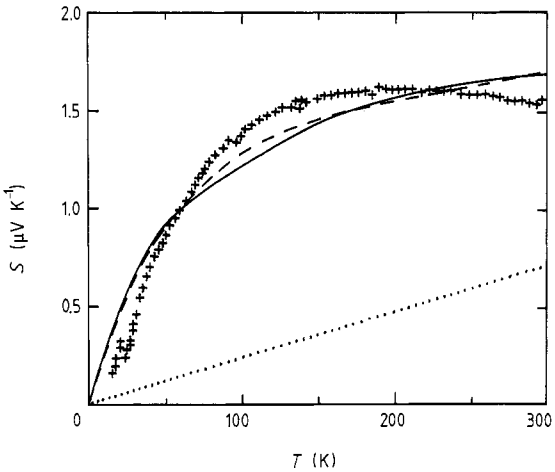

Figure 5. A comparison of the experimental data for the most nearly stoichiometric film (crosses) with the theoretical expression (3.4). The broken curve gives the best fit obtained using the Kihlstrom data; the full curve is based on the model α^2F. The dotted line shows the corresponding linear diffusion thermopower for the fit using the model α^2F.

accounted for by the energy renormalisation term $X_b\lambda$ in equation (3.5) alone: $X_B\lambda$ is approximately 5 nV K^{-2} using $\lambda = 1.46$ and approximately 3 nV K^{-2} using $\lambda = 1.19$—in both cases much smaller than the deduced values of c. This suggests a role for the velocity and relaxation renormalisation term 2α and/or the higher-order-diagram term γ, with $2\alpha + \gamma$ of order 9 nV K^{-2} (Kihlstrom data) and 14 nV K^{-2} (model α^2F). These values of $2\alpha + \gamma$ are of similar order of magnitude to that expected theoretically and found for Ni–Zr (Kaiser 1984) and Ag–Sn films (Compans 1987) (the value for the Ag–Sn films, however, is negative, as predicted for α in the case of nearly free-electron systems). We cannot distinguish between velocity and relaxation time renormalisation and higher-order diagrams as regards which is dominant in NbN. This is because the positive value of X_b implies that nearly free-electron behaviour cannot be assumed, so the sign of α expected theoretically cannot realistically be determined (γ is generally expected to be positive (Kaiser and Stedman 1985)).

Whether α or γ contributes most to the positivity of $2\alpha + \gamma$ cannot be determined in the present case. It is because the bare thermopower $S_b(T)$ is small in NbN that the energy renormalisation effect is small and the other terms, therefore, much more important in determining the temperature dependence of the thermopower.

In systems with large thermopowers the energy renormalisation effect alone is usually adequate for accounting for the observed behaviour (Kaiser *et al* 1986, Kaiser 1987a).

We note that the deduced value of $2\alpha + \gamma$ is probably an overestimate because of the apparent presence of an additional effect causing the decrease in thermopower slope below that expected at higher temperatures. The assumption that the parameter X_b is constant, i.e. that the bare thermopower is linear, is in fact an approximation, since there are other effects that may cause temperature dependence of the thermopower parameter.

For example, changes in the structure in the Ziman–Faber model could affect the thermopower as well as the resistivity. In general, these changes would be expected to be rather slow at low temperatures, so the dominant effect at low temperatures is still

expected to be due to the electron–phonon interaction. However, these other effects could cause a tendency for the thermopower to show a small but increasing curvature at higher temperatures, which would be especially evident for cases where the thermopower is small, as in NbN.

4. Conclusions

Applying a recently developed dynamic technique, the absolute thermoelectric power $S(T)$ of NbN films prepared by DC sputtering was determined as a function of temperature within the range $7.2\ \mathrm{K} \leqslant T \leqslant 300\ \mathrm{K}$. Although the detailed shape of $S(T)$ is influenced by stoichiometry variations, the sign of S is always found to be positive.

The pronounced non-linear $S(T)$ behaviour can be explained as being due to electron–phonon renormalisation effects. In arriving at this conclusion the experimental results were fitted to the corresponding theory using experimentally determined Eliashberg functions and satisfactory agreement was obtained.

Acknowledgments

We would like to thank Dr E Compans for much useful advice concerning the dynamical technique, Dr U Kaufmann for the preparation of the films and Dr J Geerk for helpful discussions on α^2F.

References

Allen P B and Dynes R C 1975 *Phys. Rev.* B **12** 905
Bacon D D, English A T, Nakahara S, Peters F G, Schreiber H, Sinclair W R and van Dover R B 1983 *J. Appl. Phys.* **54** 6509
Brauer G and Kirner H 1964 *Z. Anorg. Allg. Chem.* **328** 34
Capone D W II, Gray K E and Kampwirth R T 1989 *J. Appl. Phys.* **65** 258
Compans E 1987 *PhD Thesis* Universität Karlsruhe
—— 1989 *Rev. Sci. Instrum.* **60** 2715
Compans E and Baumann F 1987 *Japan. J. Appl. Phys.* **26** 805
Dacorogna M, Jarlborg T, Junod A, Pellizone M and Peter M 1984 *J. Low. Temp. Phys.* **57** 629
Darlinksi A and Halbritter J 1987 *Surf. Interface Anal.* **10** 223
Egorushkin V E and Melnikova N V 1987 *J. Phys. F: Met. Phys.* **17** 2389
Gallagher B L 1981 *J. Phys. F: Met. Phys.* **11** L207
Geerk J, Linker G and Smithley R 1986 *Phys. Rev. Lett.* **57** 3284
Geerk J, Schneider U, Bangert W, Rietschel H, Gompf F, Gurvitch M, Remeika J and Rowell J M 1985 *Physica* B **135** 187
Gompf F and Reichardt W 1975 *Progress Report of the Teilinstitut für Nukleare Festkörperphysik* ed. L Pintschovius (Karlsruhe: Gesellschaft für Kernforschung)
Jäckle J 1980 *J. Phys. F: Met. Phys.* **10** L43
Kaiser A B 1982 *J. Phys. F: Met. Phys.* **12** L223
—— 1984 *Phys. Rev.* B **29** 7088
—— 1987a *Phys. Rev.* B **35** 4677
—— 1987b *Phys. Rev.* B **35** 2480
Kaiser A B, Christie A L and Gallagher B L 1986 *Aust. J. Phys.* **39** 909
Kaiser A B and Stedman G E 1985 *Solid State Commun.* **54** 91
Kihlstrom K E, Simon R W and Wolf S A 1985 *Phys. Rev.* B **32** 1843
Lye R G 1965 *J. Phys. Chem. Solids* **26** 407

L'vov S N, Nemchenko V F and Samsonov G V 1960 *Sov. Phys.–Dokl.* **135** 1334
Mawdsley A and Kaiser A B 1988 *Solid State Commun.* **66** 1023
McMillan W L and Rowell J M 1969 *Superconductivity* vol 1, ed. R D Parks (New York: Marcel Dekker)
Naugle D G, Delgado R, Armbrüster H, Tsai C L, Johnson W L and Williams A R 1985 *J. Phys. F: Met. Phys.* **15** 921
Nigro A, Nobile G, Rubino M G and Vaglio R 1988 *Phys. Rev.* B **37** 3970
Ono Y A and Taylor P L 1980 *Phys. Rev.* B **22** 1109
Reiff S 1988 *Diploma Thesis* Universität Konstanz
Roberts R B 1977 *Phil. Mag.* **36** 91
Samsonov G V and Verkhoglyadova T S 1962 *Dokl. Akad. Nauk SSSR* **142** 608